An Analytical Model for the Motion and Radiative Response of a Low Density Inertial Confinement Fusion Buffer Gas

T.J. McCarville, G.L. Kulcinski, and G.A. Moses

January 1981

UWFDM-405

FUSION TECHNOLOGY INSTITUTE

UNIVERSITY OF WISCONSIN

MADISON WISCONSIN

An Analytical Model for the Motion and Radiative Response of a Low Density Inertial Confinement Fusion Buffer Gas

T.J. McCarville, G.L. Kulcinski, and G.A. Moses

Fusion Technology Institute
University of Wisconsin
1500 Engineering Drive
Madison, WI 53706

http://fti.neep.wisc.edu

January 1981

UWFDM-405

An Analytical Model for the Motion and Radiative Response of a Low Density Inertial Confinement Fusion Buffer Gas

T. J. McCarville

G. L. Kulcinski

G. A. Moses

Fusion Engineering Program
Nuclear Engineering Department
University of Wisconsin
Madison, WI 53706

January 1981

UWDFM-405

Introduction

Most cavity designs that have been proposed for inertial confinement fusion anticipate a background gas or vapor in the chamber originating from one source or another. The atom density might range anywhere from about 3.5×10^{12} atoms/cm^3 (10^{-4} Torr at 273°K) for heavy ion beam drivers, up to about 3.5×10^{18} atoms/cm^3 (100 Torr at 273°K) for light ion beam drivers. Although the response of a high density gas to a pellet explosion has already been studied[1], the response of a low density gas has not been adequately assessed because the methods of analysis used for a high density gas are inappropriate. The purpose of this report is to describe some of the tools necessary to analytically predict the radiation transport and gas motion of a low density gas in an ICF chamber.

The definition of a low density gas as the term is used here refers to a gas that is transparent enough to radiation that gradients in the radiation energy density relax faster than gradients in the gas pressure, i.e., a front of radiation travels faster than the speed of sound. This condition precludes the use of Taylor's[2] theory of shock waves because the radiation energy becomes decoupled from the gas motion. With this decoupling, the conditions required for a blast wave are not met and the only significant gas motion is from the momentum imparted by the debris. Momentum conservation is used in this study to derive a simple expression for the gas motion that applies if the debris pushes on the gas like a piston. The parameters that determine whether the debris will push on the gas like a piston or simply stream through it are identified and the analysis is carried further using energy conservation to derive an expression for the heat flux originating from the debris driven shock. When the gas and debris satisfy the conditions that are

outlined below, the expressions presented here can provide a first estimate of the gas motion and heat flux.

Computations from the analytic expressions derived here are compared to a numerical solution of the radiation hydrodynamics equations that includes the interaction of the expanding pellet with the gas. The numerical solution provides a greater degree of detail than the analytic equations but is relatively expensive to use. The equations derived here are only meant to provide first estimates of the gas motion and heat flux, as well as indicate general trends.

Conservation of Momentum

When the pellet is in a compressed, high temperature state, a fraction of the thermonuclear energy released by the fuel is manifested in internal energy. This internal energy is quickly converted to kinetic energy as the pellet expands with what is assumed to be spherical symmetry. The average radial momentum of the expanding debris, $m_d u_d$, varies with time due to interactions with cavity gas atoms. It follows from momentum conservation that

$$m_d u_{do} = m_d u_d + m_g u_g \qquad (1)$$

where u_{do} denotes the initial debris speed and $m_g u_g$ is the momentum transferred to the gas. It is assumed here that the momentum imparted to the gas causes the debris to act as a spherically expanding piston, pushing ahead a compressed layer of gas as shown in Figure 1. If the debris does not penetrate very far into the compressed gas then the speed of the compressed gas layer, u_g, is nearly equal to that of the debris, or

$$u_g = u_d = \dot{r} \quad , \qquad (2)$$

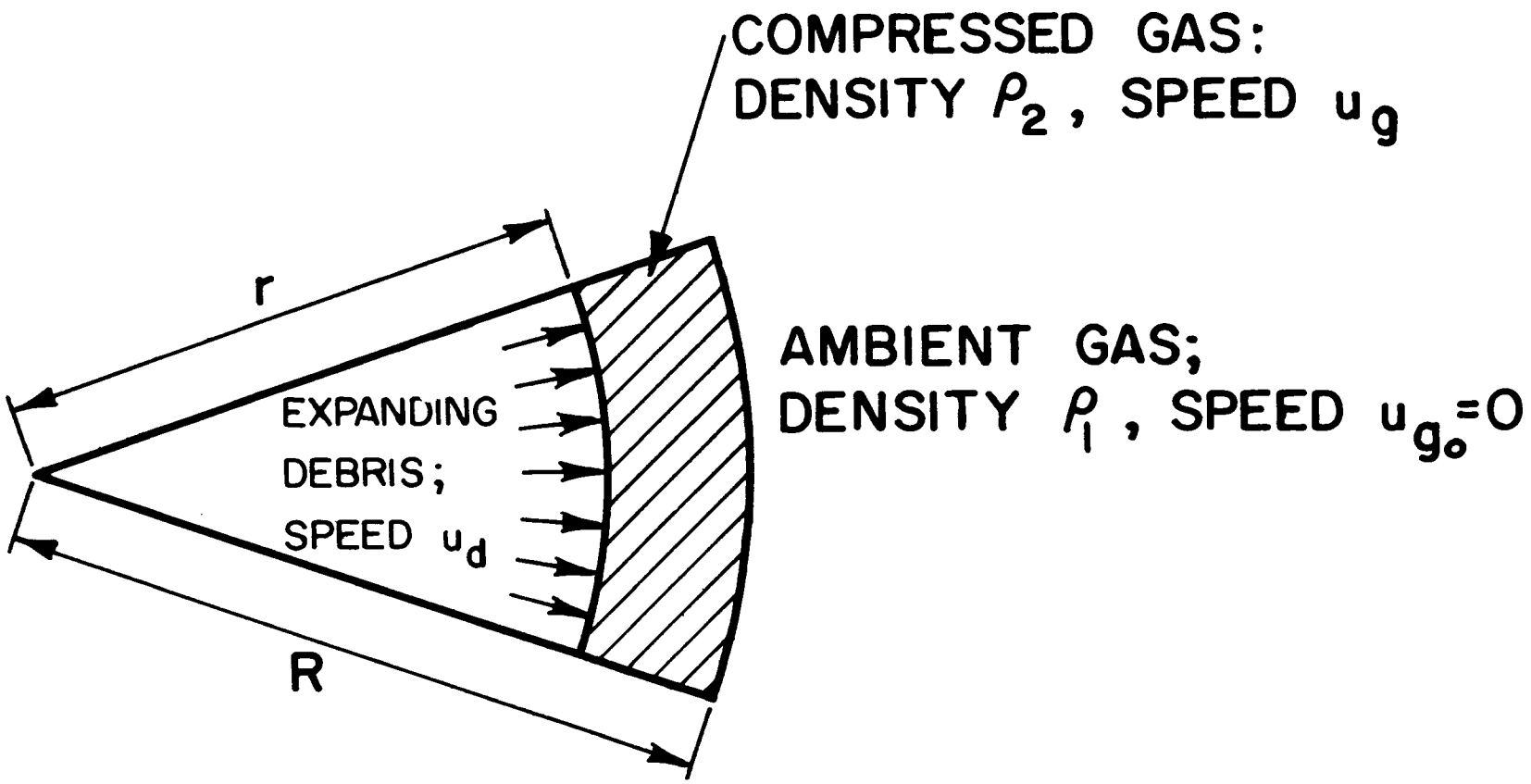

Figure 1. A cross section of the ambient gas, compressed gas, and expanding debris layers.

where $\dot{r}$ is the speed of the debris-compressed gas interface.

The speed of the ambient gas-compressed gas interface, $\dot{R}$, will now be expressed as a function of $\dot{r}$. As the pellet begins to expand, $\dot{R}$ will be much greater than the sound speed of the gas, implying R is the position of a strong shock. The Hugoniot equation for a strong shock in a perfect gas with constant specific heats requires that

$$\frac{\rho_2}{\rho_1} = \frac{\gamma+1}{\gamma-1} \quad , \tag{3}$$

where γ is the ratio of specific heats. Writing conservation of mass flux across the shock front as

$$\rho_1 \dot{R} = \rho_2 (\dot{R} - \dot{r}) \quad , \tag{4}$$

and combining this with Eq. (3), the speed of the debris-compressed gas interface can be related to shock speed by

$$\dot{r} = \frac{2}{\gamma+1} \dot{R} \quad . \tag{5}$$

Since γ is always greater than one, $\dot{R}$ is always greater than $\dot{r}$.

The last relation required to solve Eq. (1) for R as a function of time is Found by noting that the mass of the compressed gas zone, m_g, is related to R by

$$m_g = \frac{4}{3} \pi R^3 \rho_1 \quad . \tag{6}$$

Now combining Eqs. (1), (2), (5) and (6), the equation for the shock speed as a function of position is found to be

$$\frac{2}{\gamma+1} \dot{R} \left[m_d + \frac{4}{3} \pi R^3 \rho_1\right] = m_d u_{do} \cdot \tag{7}$$

As the debris sweeps out an increasing mass of gas, the shock strength will weaken, meaning the pressure ratio across the shock front will decrease. Equation (3) becomes invalid for weak shocks, causing Eq. (7) to incorrectly predict that $\dot{R}$ will eventually become less than the speed of sound, c. It would seem desirable to extend this analysis to include weak shocks by using the general form of the Hugoniot equation instead of Eq. (3). Unfortunately, the general form introduces algebraic complexities that make it impossible to express $\dot{r}$ explicitly in terms of $\dot{R}$, as was done in Eq. (5). Hence, it is only possible to find an analytic description of the gas motion as long as the pressure ratio across the shock front is greater than ten, so that Eq. (3) holds true.

As long as $\dot{R}$ is much greater than the sound speed, the shock position as a function of time is found by integrating Eq. (7), resulting in

$$\frac{2}{\gamma+1} \frac{R}{u_{do}} \left[1 + \frac{\pi}{3} R^3 \frac{\rho_1}{m_d}\right] = t \cdot \tag{8}$$

An alternative description of the response of a low density gas to the pellet expansion was given by Freiwald and Axeford.[5] That analysis extends the range of Taylor's blast wave theory to low density gases by including the pellet mass in the analysis. However, Taylor's approach applies only if the gas motion has the property of self-similarity, meaning the partial

differential equations of mass, momentum, and energy conservation can be reduced to a single, ordinary differential equation by a transformation to similarity variables. A suitable similarity variable will not exist if the shock is transparent to the radiation emitted by the zone of compressed gas, and a self-similar blast wave will not form. If the shock is transparent to the emitted radiation, then the gas motion is best described by Eq. (8).

A parameter in Eq. (8) that is often difficult to specify is the adiabatic constant, γ, which is temperature dependent. A monatomic gas with only translational degrees of freedom has γ equal to 5/3. At higher temperatures the ratio of ionization to translational energy increases and γ decreases to a value between 1 and 5/3. At even higher temperatures, where ionization energy is again small compared to translational energy, γ once again approaches 5/3. Since photons emitted by the pellet heat the cavity gas before the shock passes through, the state of the gas must be estimated before choosing γ. Knowing the bounds on the value that γ can have, the maximum error in computing the shock position from Eq. (8) that can be made by an improper choice of γ is no greater than 25% for a monatomic gas.

The value chosen for γ can strongly affect the reflected overpressure computed at the wall, P_r. For strong shocks one finds P_r is related to the pressure of the compressed gas layer, P_2, by[6]

$$P_r = \frac{3\gamma-1}{\gamma-1} P_2 \quad . \tag{9}$$

Equation (9) can have an uncertainty greater than 100% if γ is not accurately known. By carefully estimating the ionization state of the gas ahead of the

shock, experience shows that the uncertainty introduced into Eq. (9) can be reduced to less than about 20%.

If the debris streams through the gas rather than acting as a spherically expanding piston then no debris driven shock wave will ensue. The parameters that influence whether the debris will drive a shock or stream through the compressed gas can be identified by first writing energy conservation as

$$\frac{1}{2} m_d u_{do}^2 = \frac{1}{2} m_d u_d^2 + \Delta KE_g + \Delta INT_g \quad , \tag{10}$$

where ΔKE_g and ΔINT_g represent the change in kinetic and internal energy of the gas, respectively. Combining Eqs. (1) and (10) reveals something about the propensity for a debris driven shock to occur, which can be studied by writing

$$\frac{\Delta INT_g}{\Delta KE_g} = \frac{m_g(u_{do}^2 - u_d^2)}{m_d(u_{do} - u_d)^2} - 1 \quad . \tag{11}$$

The ratio on the left hand side will have a value near zero if there is a debris driven shock, and values around one or greater if the debris stream through the gas. The mass of gas through which the debris will traverse, m_d, can be computed from the final range of the pellet ions in the gas, r^*. At the end of range, $u_d = 0$ and Eq. (11) becomes

$$\frac{\Delta INT_g}{\Delta KE_g} = \frac{4\pi\rho_1 r^{*3}}{3\, m_d} - 1 \quad . \tag{12}$$

Thus the pellet mass, gas density, and projected range of the debris can be used to deduce whether or not a debris driven shock will occur. The value of

the range, r^*, used in Eq. (12) should be that computed for a projectile slowing down in a stationary gas. If the ratio on the right hand side of Eq. (12) is much less than one or negative (negative values imply outward radial deformation of the gas has extended the range beyond the value chosen), then a debris driven shock can be expected.

Energy Conservation

Assuming the expanding debris forms a debris driven shock, an expression for the heat flux emitted by the shock heated gas, $\dot{q}$, will now be derived with the aid of the volume element shown in Figure 2. The Newtonian reference frame of the element is fixed to the shock front. The following derivation makes use of the fact that the rate of change of the shock speed is small compared to the deceleration of the gas passing through the shock front. This assumption permits a steady state analysis.

Conservation of energy in the element requires that

$$\dot{q} = (e_1 + \frac{P_1}{\rho_1} + \frac{1}{2}\dot{R}^2)\,\rho_1\dot{R} - (e_2 + \frac{P_2}{\rho_2} + \frac{1}{2}(\dot{R} - \dot{r})^2)\,\rho_2\,(\dot{R} - \dot{r}), \quad (13)$$

where e denotes specific internal energy and the subscripts denote the properties in regions 1 and 2 shown in Figure 2. Equations (3), (4) and (5) reduce Eq. (13) to

$$\dot{q} = [\frac{2}{(\gamma+1)}\dot{R}^2 + (e_1 + \frac{P_1}{\rho_2} - e_2)]\,\rho_1\dot{R}\,. \quad (14)$$

If the shock front is opaque to radiation emitted by the zone of compressed gas, then $\dot{q}$ is negligible and Eq. (14) relates e_2 to $\dot{R}$. The temperature profile of the gas is shown in Figure 3(a) for such a shock, which is

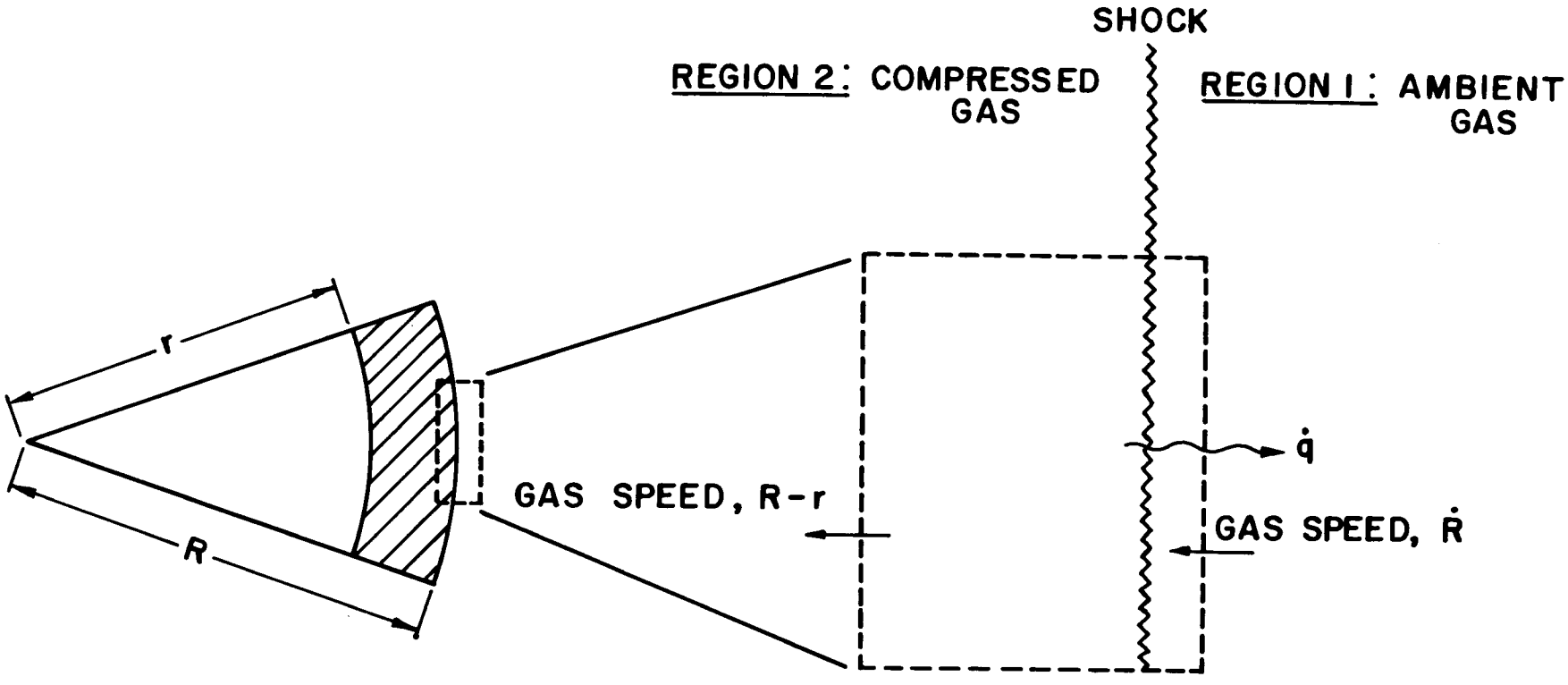

Figure 2. The volume element chosen for the energy analysis is outlined above. The element is stationary in a coordinate system fixed to the shock.

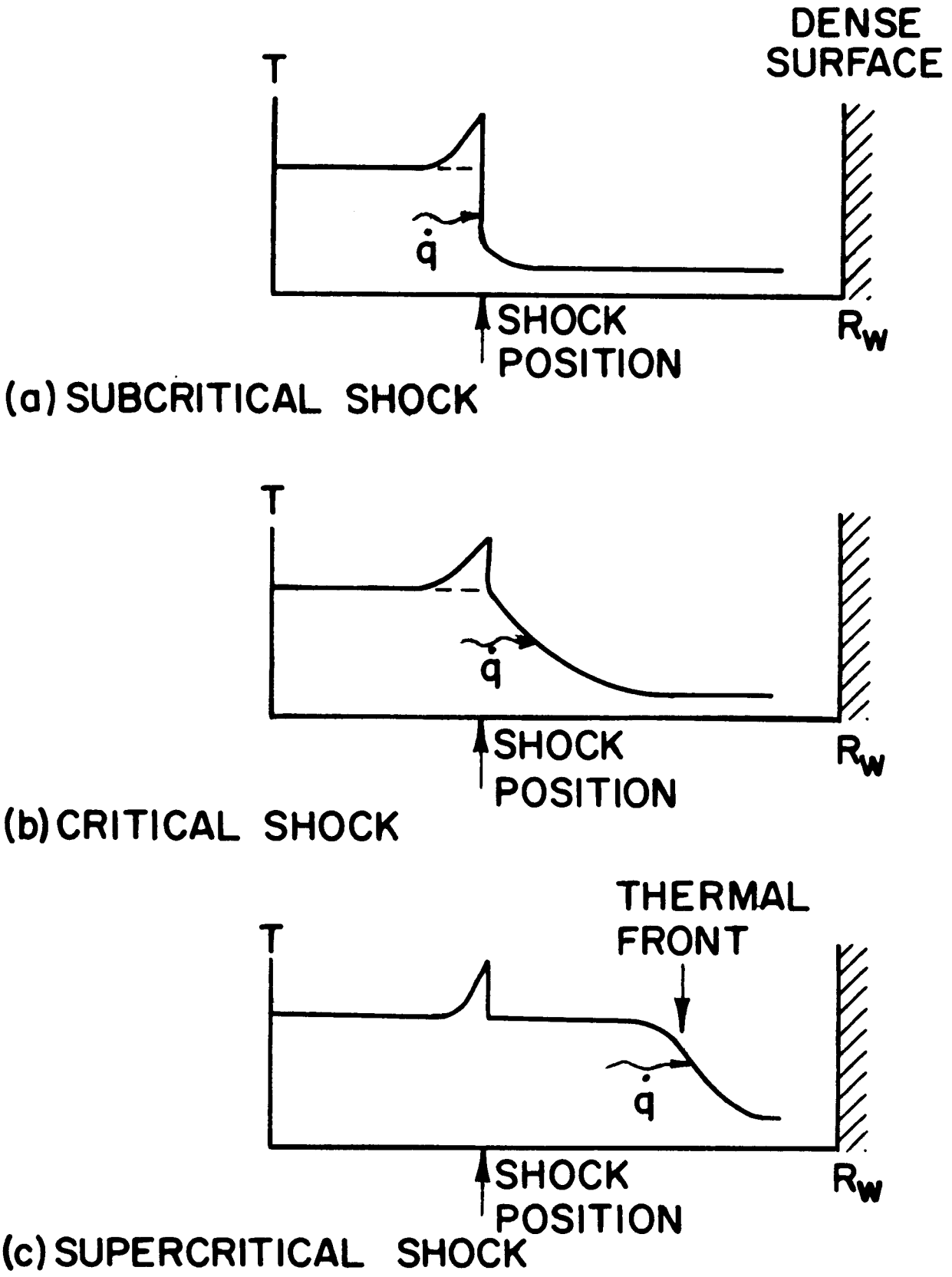

Figure 3. Temperature profiles for a: (a) subcritical, (b) critical, (c) supercritical shock wave. These profiles illustrate the trend of radiation transport in a high density, intermediate density, and low density gas, respectively.

referred to as a subcritical shock. Taylor's blast wave theory or Freiwald and Axeford's extension of that theory is applicable to subcritical shocks. If the shock is not quite opaque, but instead is partially transparent to some of the radiation, then none of the terms in Eq. (14) can be neglected. This occurs when the radiation mean free path at the shock front is larger than about a fraction of a centimeter. The temperature profile for this case may look like that shown in Figure 3(b), which is called a critical shock because radiation has heated the gas temperature ahead of the shock to the temperature behind the shock. A detailed analysis of this case requires an equation of state for the gas, a radiation transport model, and a computer to solve the radiation hydrodynamics equations.

There is yet a third "mode" for Eq. (13), one that will apply to debris driven shocks that are completely transparent to radiation emitted by the gas. The temperature profile for this type of shock, which is called a supercritical shock, is seen if Figure 3(c). Since the internal energy of the compressed gas zone is negligible compared to its kinetic energy then the term involving $\dot{R}$ can dominate the right-hand-side of Eq. (14), leaving

$$\dot{q} \approx \frac{2}{(\gamma+1)^2} \rho_1 \dot{R}^3 \quad . \tag{15}$$

Equation (15), which can be evaluated using Eq. (8), can be used to compute the heat flux at the wall once the thermal front has reached that point. For a spherical wall positioned at R_w, the heat flux from the shock is

$$\dot{q} = \frac{2}{(\gamma+1)^2} \rho_1 \dot{R}^3 \left(\frac{R}{R_w}\right)^2 \quad . \tag{16}$$

The concepts and expressions developed thus far will now be illustrated by way of examples.

Examples

The expressions describing the motion and heat flux of a debris driven shock will be compared to a numerical solution of the radiation-hydrodynamic equations that includes the effects of the debris-gas interaction. A description of the FIRE code used for the numerical solution is given elsewhere.[3]

An argon cavity gas that contains 0.2 atomic percent Na and a density of 10^{15} atoms/cm^3 (2.8×10^{-2} Torr at 273°K) was chosen for the examples presented here. A total of 15 MJ of 0.3 keV blackbody x-rays was assumed for the spectra of pellet photons. The resulting energy deposition profile in a 4 meter, spherical cavity is shown in Figure 4. The temperature profile of the gas, also shown in Figure 4, was computed using the FIRE code and an equation of state for the gas.[7] γ, the adiabatic exponent, was estimated using

$$\gamma = 1 + \frac{P_1}{\rho_1 e_1} ,$$

where the thermodynamic parameters were evaluated after the deposition of pellet photons. The average value of γ throughout the cavity is about 1.12 for this example, and the average charge state of the gas atoms is on the order of +1.

The x-ray deposition calculation showed that only 2.5 MJ of the pellet photon energy is absorbed by the gas. The unattenuated photons are absorbed within the first few microns of first wall material over a time on the order of one to tens of nanoseconds. The resulting heat flux is hundreds of megawatts per square centimeter (6.2 J/cm^2).

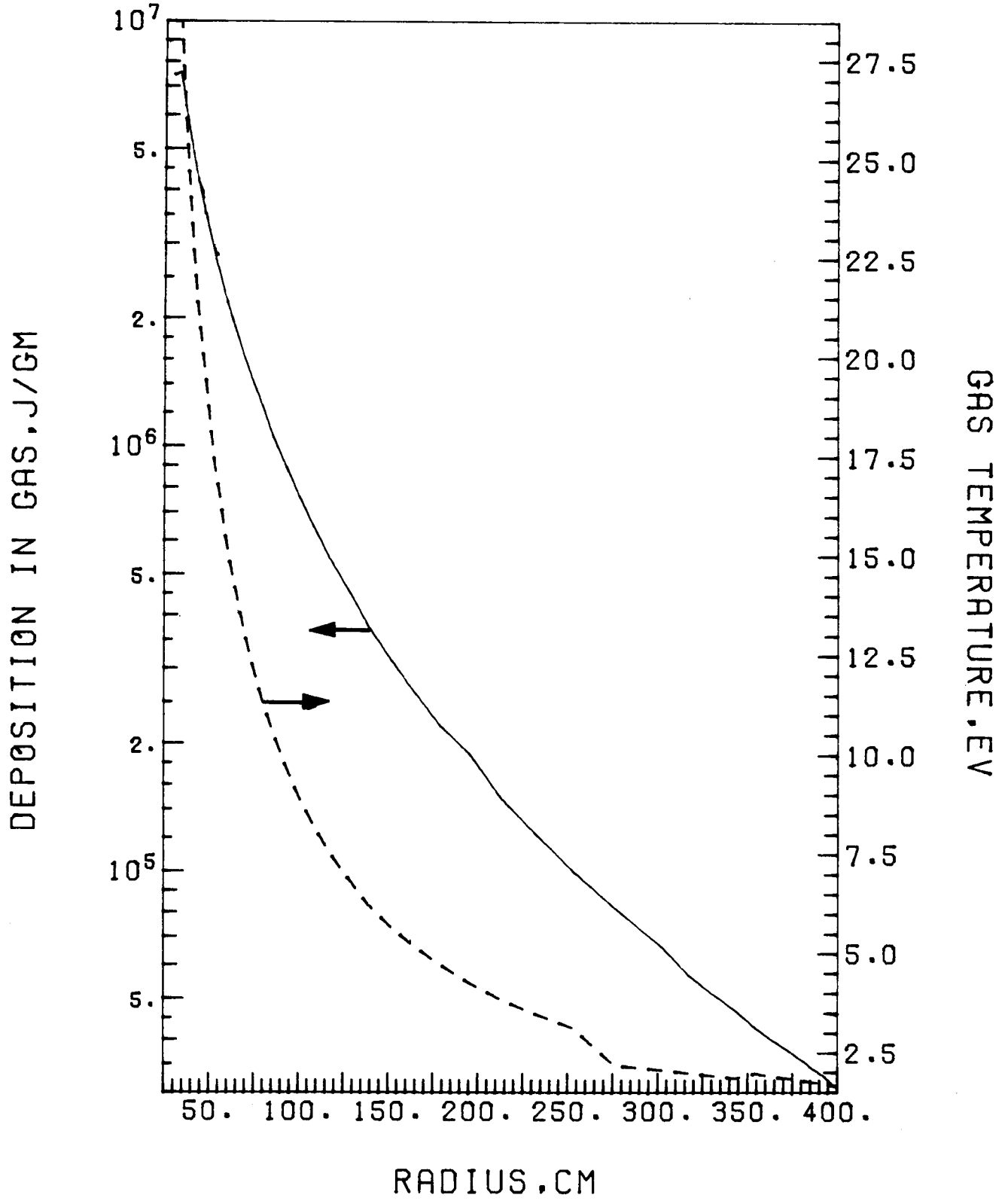

Figure 4. The energy deposition and temperature profile from the FIRE code for 15 MJ of 0.3 keV blackbody x-rays passing through argon gas with 10^{15} atoms/cm^3. The x-rays originate at the center of a 4 meter, spherical cavity.

The pellet debris chosen to illustrate the use of the analytic expressions derived in this work is one gram of iron possessing 15 MJ of the thermonuclear energy released. The energy of each debris ion is 15 keV. From the gas density, pellet mass, and an estimate of the debris range in the Argon gas, (71 cm), Eq. (12) can be used to predict the likelihood of a debris driven shock. For the parameters given above the ratio of internal to kinetic energy computed by Eq. (12) is negative, implying a debris driven shock will occur. Predictions of the shock position as a function of time from Eq. (8), the FIRE code, and reference (5) are compared in Figure 5. Equation (8) initially predicts a swifter shock than the FIRE code because its derivation assumes all the debris energy goes directly into kinetic energy of the gas, whereas the numerical solution accounts for the small fraction that goes into internal energy. The internal energy component becomes part of the supercritical wave of radiation radiated ahead of the shock, and is not coupled to the shock motion. At later times Eq. (8) predicts a slower shock than the FIRE code because it fails to limit the speed of the disturbance to the sound speed, c, which the FIRE code estimates to be 3×10^5 cm/sec at the wall. Equation (7) predicts the shock speed at the wall will be twice this value, which is close enough to c to expect that Eq. (7) will underestimate the shock speed. Figure 5 shows how this results in an overestimation of the time to reach the wall by 20% when compared to the numerical solution. This difference is carried into the reflected overpressure calculation, which is 0.62 atmospheres from the analytic equations, and 0.82 atmospheres from FIRE. The FIRE code predicts the duration of the shock reflection at the wall is on the order of 10^{-5} seconds.

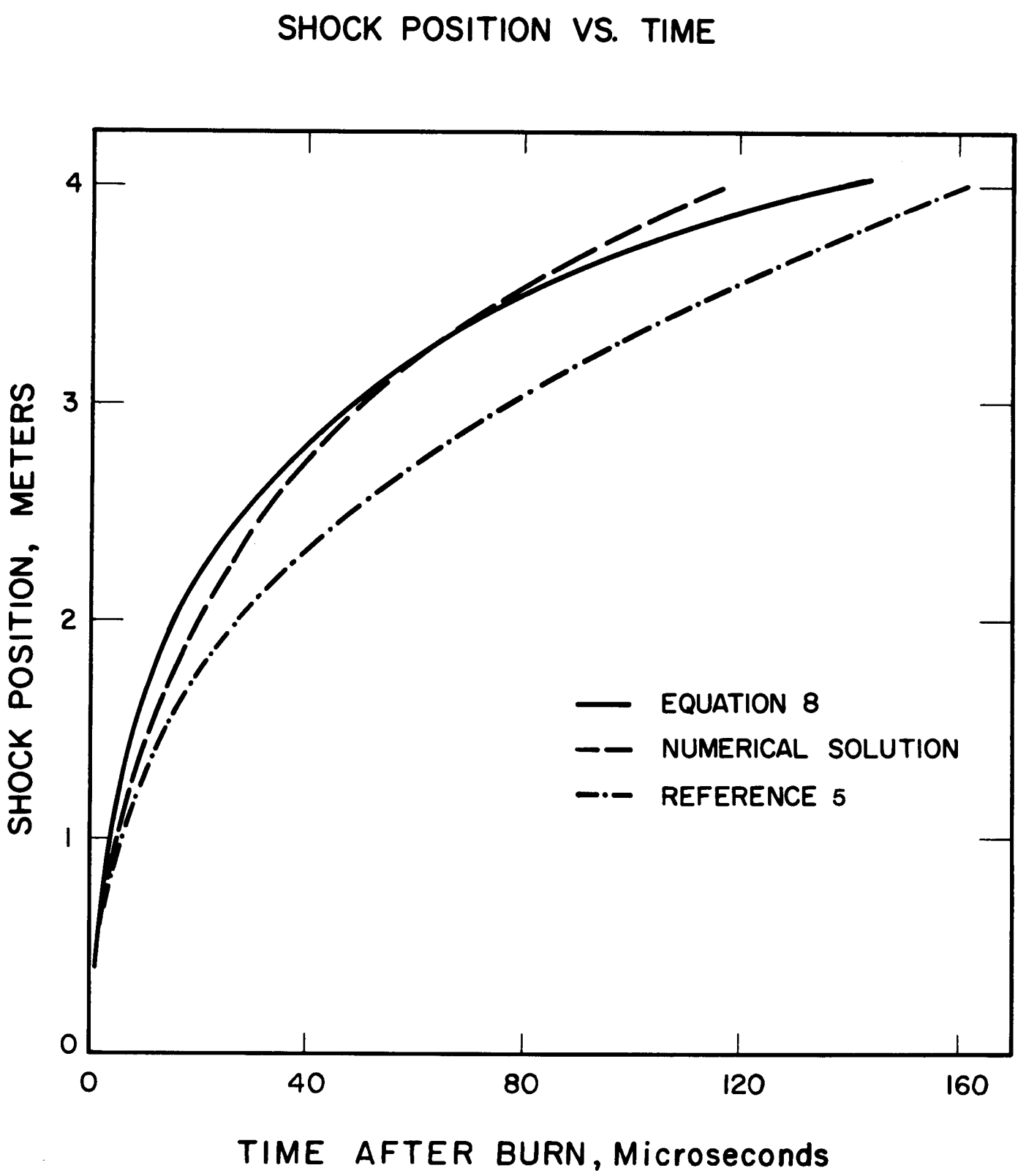

Figure 5. The shock position as a function of time for three proposed methods of analysis.

The FIRE calculation revealed that for the gas density chosen in this example the radiation front emitted by the gas moves at a speed much greater than the debris driven shock. The radiation front reaches the wall about 10^{-7} seconds after the debris begins its expansion, and the gas is transparent to any subsequent radiation. Figure 6 shows the heat flux passing through the shock as computed from Eq. (15) and also from the FIRE code. At small times the assumption that the kinetic energy term in Eq. (14) dominates over the internal energy term breaks down, so Eq. (15) overestimates the heat flux. But for most of the time that the debris drives the shock the two heat flux curves show the same general behavior. At larger times the numerically computed flux is greater than that from Eq. (15) because the FIRE code accounts for the fraction of the debris energy that goes directly into internal energy of the gas, which is then rapidly radiated to the wall. Equation (15) assumes all of the debris energy has gone into shock motion.

Figure 7 shows the heat flux at the wall as computed from Eq. (16) and also from the FIRE code. The reasons for the differences between the two calculations that were given for Figure 6 also apply to Figure 7. Figure 7 also shows the heat flux during reflection of the shock, where, according to the FIRE code, almost 2 MJ were radiated to the wall. Equation (16) is valid from the time it takes the debris to expand out to one meter up until the shock reflects off the wall, or from 7×10^{-6} s to 1×10^{-4} s. Analytic expressions to describe the radiation emitted by a reflected shock have not yet been developed.

As a second example of the gas response to a pellet explosion, the pellet mass of the first example was reduced by a factor of 10 down to 0.1 gm while all other parameters remained the same. The energy per projectile is now 150

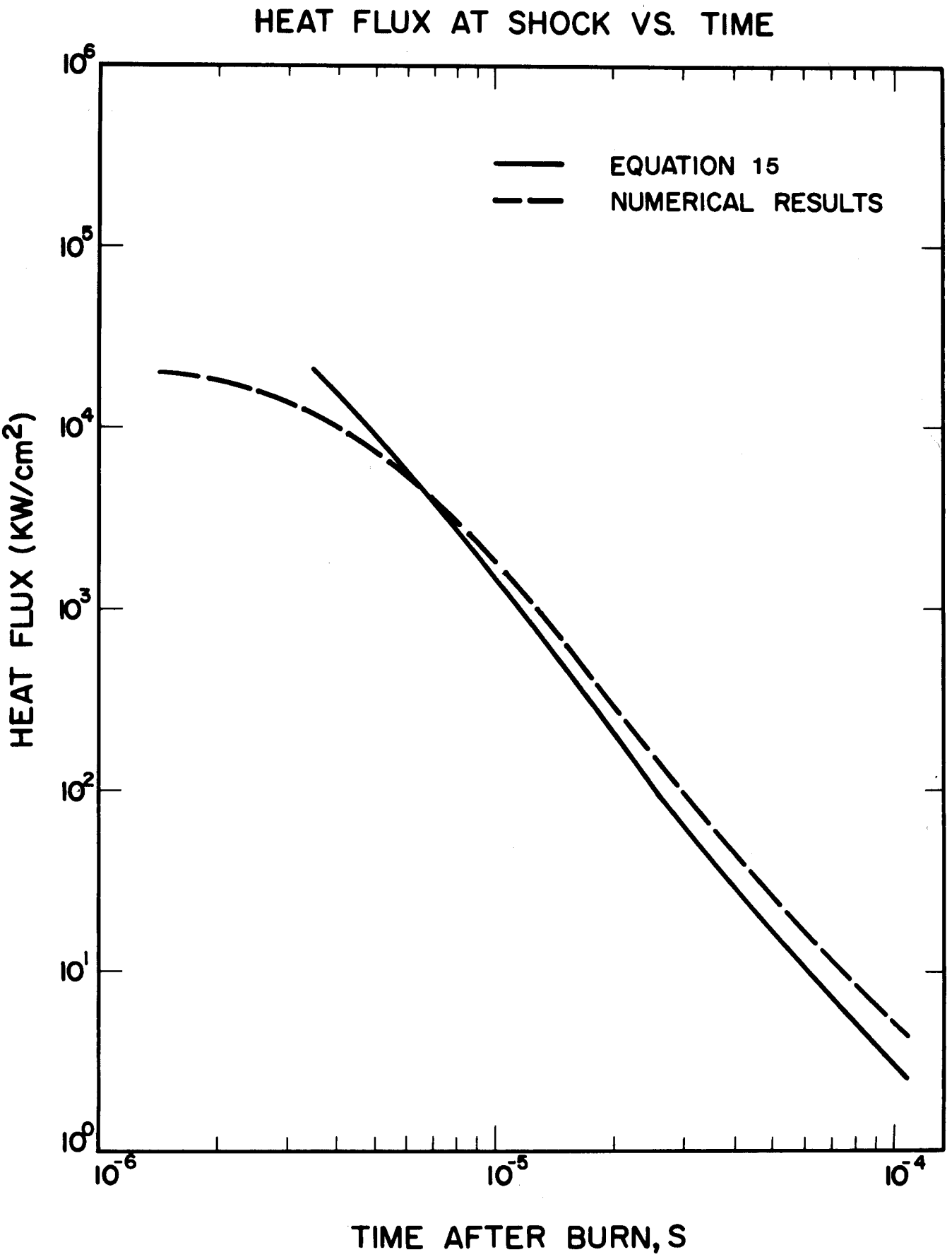

Figure 6. The heat flux emitted from the surface of the shock as a function of time.

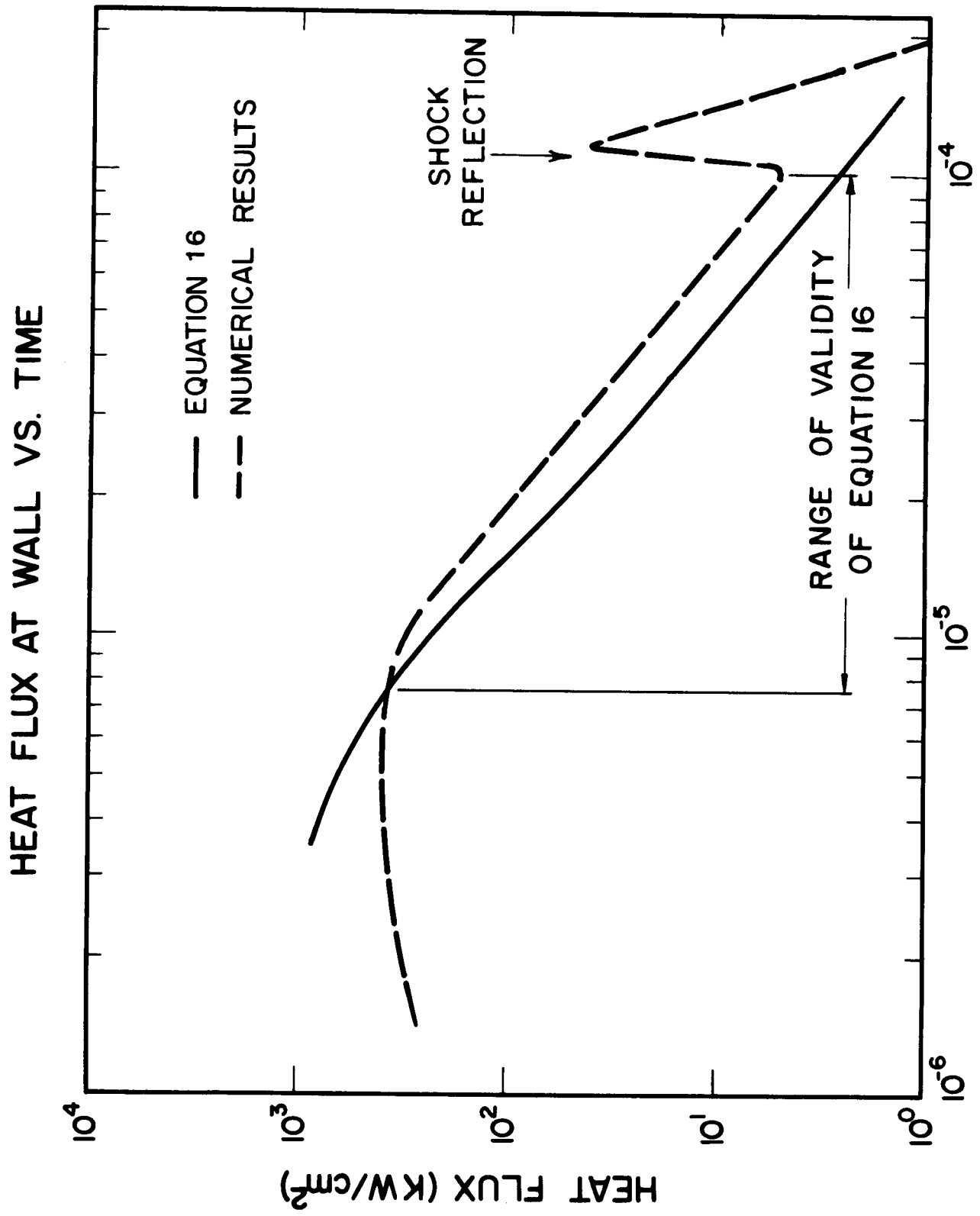

Figure 7. The heat flux at the wall as a function of time.

keV and the range, assuming the gas is stationary, is 225 cm. The ratio of internal to kinetic energy of the gas computed from Eq. (12) is one hundred, so the expanding pellet debris will lose most of its energy while streaming through the gas. In order to bring to light the difference that streaming makes, this section will close by comparing the gas response to the two example pellets. Since the analytic expressions will not accurately predict the gas response to the explosion of the 0.1 gram pellet, the FIRE code was used for the comparison.

Figures 8(a) and 8(b), which show how zones of constant mass deform with time, are FIRE results comparing the gas motion induced by the two spectra. A shock begins to form as the 0.1 gm pellet expands, but after about 10^{-7} s the debris streams through and the shock quickly loses its energy.

The cumulative energy deposited into the gas by the two pellets is compared in Figures 9(a) and 9(b). The curve for the 0.1 gram pellet rises more rapidly with time due to the greater speed of the debris ions. Also shown in Figures 9(a) and 9(b) is the energy retained by the gas. The kinetic energy imparted to the gas by the 1.0 gram pellet is retained longer than the internal energy deposited by the 0.1 gram pellet, but with time the kinetic energy is eventually converted to internal energy as the debris driven shock heats the gas.

Figure 10 shows how the difference between the two spectra affect the heat flux at the wall. The heat flux is initially greater for the 0.1 gram pellet since those debris ions increase the internal energy of the gas, which subsequently radiates, at a greater rate. But after about 6×10^{-6} seconds the heat flux is greater for the 1.0 gram pellet because the kinetic energy of the shock wave is still being converted to radiation. After the heat flux

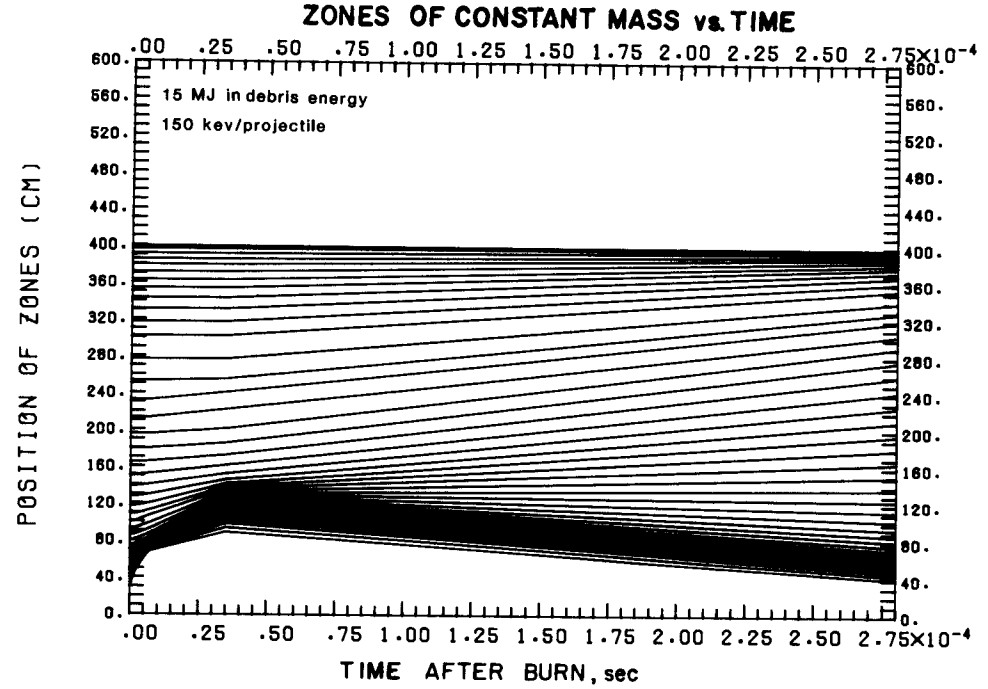

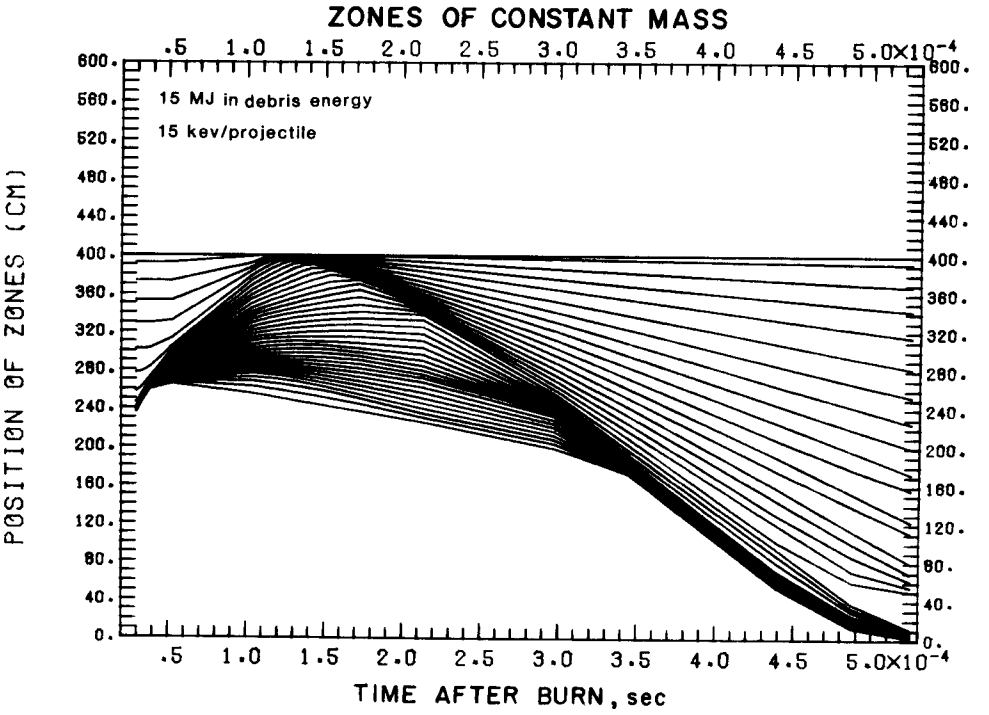

Figures 8(a) and 8(b). Zones of constant mass shown deforming with time as computed by the FIRE code. The line density is an indication of the degree of compression.

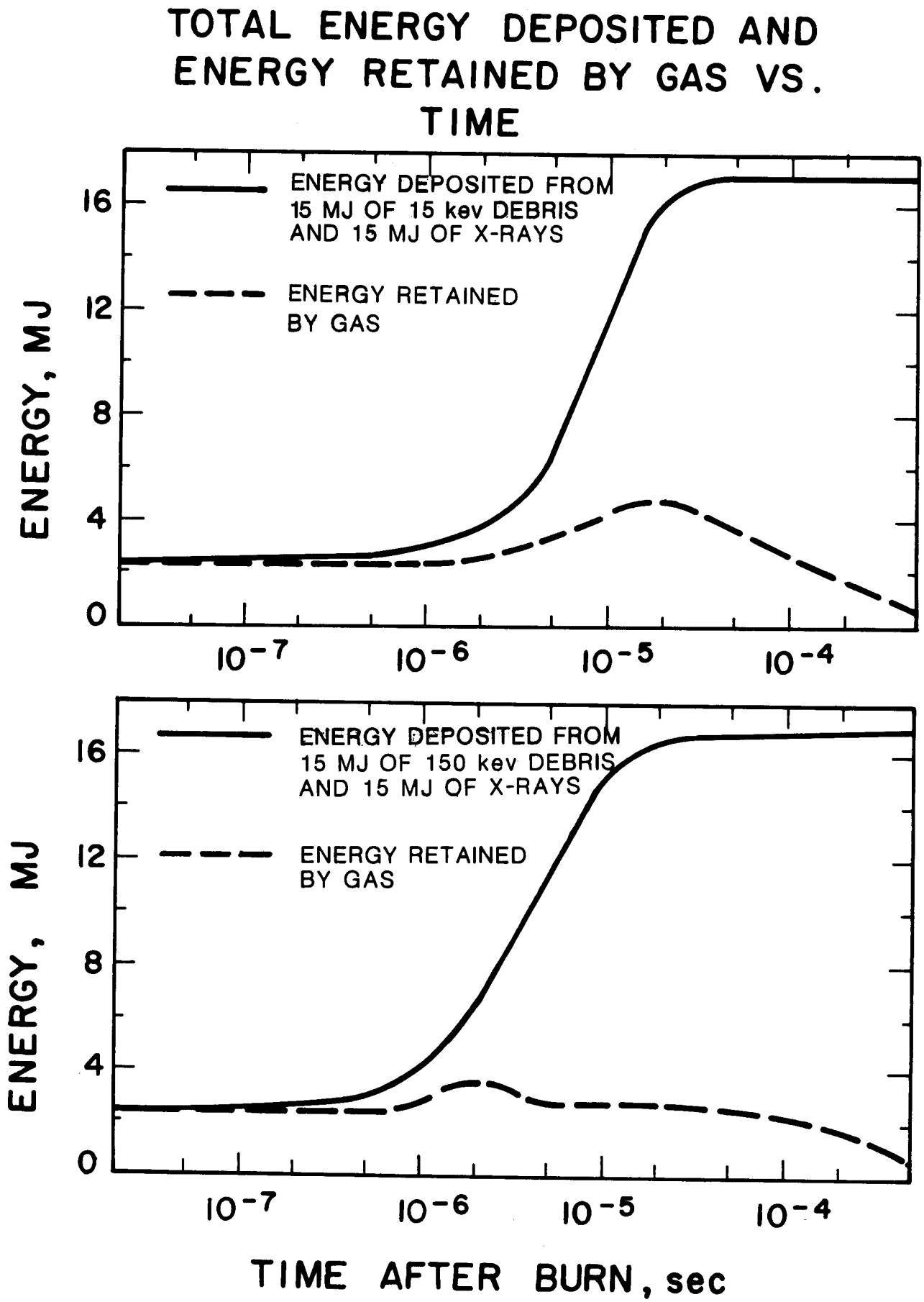

Figures 9(a) and 9(b). The energy deposited in and the energy retained by the gas as a function of time for the 15 keV debris and 150 keV debris. The FIRE code was used for this calculation.

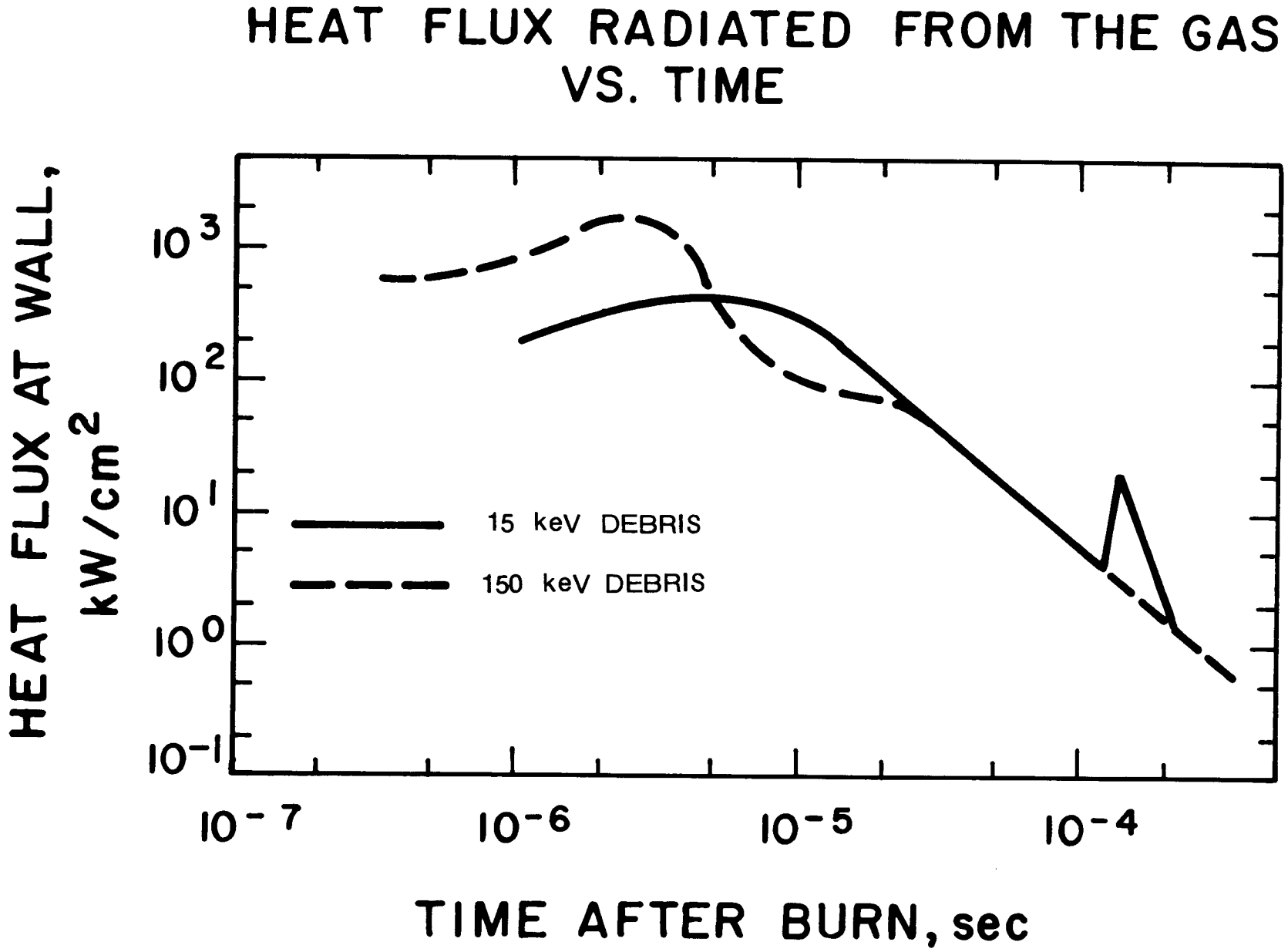

Figure 10. The heat flux at the wall as a function of time for the two spectra computed with the FIRE code.

reduces to about 50 kW/cm^2, the two curves are largely the same until the shock wave driven by the 1.0 gram pellet strikes the wall.

Summary

The primary assumptions used to derive the analytic expression of the debris driven shock as a function of time are now summarized:

- the debris-gas interface must equal the debris speed; i.e., the debris must not stream through the gas.
- the debris-gas interface must be moving much faster than the speed of sound.
- the gas must behave as a perfect gas with constant specific heat.

The first two assumptions will not always hold true, as seen in the examples. The third assumption should not cause errors greater than a few percent.

The following additional assumptions were used to derive the analytic expression for the heat flux emitted from the shock:

- a quasi-steady state analysis can be applied to the shock front.
- the shock must be transparent to radiation emitted from the heated gas.
- the internal energy of the compressed gas must be a small fraction of its kinetic energy.

The assumption of a quasi-steady state is valid for shocks not undergoing reflection and the assumption of transparency to radiation should hold true for the low density gases being considered here. Finally, if the shock is transparent to radiation, then the kinetic energy of the debris driven gas layer may be much smaller than the internal energy, and the analytic expression describing the heat flux emitted by the gas will be applicable.

Acknowledgment

This work was supported by Sandia Laboratories under contract #13-9838.

References

1. R.R. Peterson, G.W. Cooper, G.A. Moses, "Cavity Gas Analysis for Light Ion Beam Fusion Reactors," Nuclear Technology, July 1981.

2. G. Taylor, Proc. R. Soc., A201, 159 (1950).

3. T.J. McCarville, G.A. Moses, R.R. Peterson, "FIRE3 - A New Approach to Computing the Cavity Gas Response in ICF Reactors". To be published.

4. YA.B. Zel'Dovich and YU.R. Raizer, Physics of Shock Waves and High Temperature Hydrodynamics Phenomena, Academic Press, 1967, Vol. I, Ch. 12.

5. D.A. Freiwald and R.A. Axeford, "Approximate Spherical Blast Theory Including Source Mass," Journal of Applied Physics, Vol. 46, No. 3, 1975.

6. L.D. Landau and E.M. Lifshitz, Fluid Mechanics, Oxford, Pergamon Press, 1959, P. 365.

7. R.R. Peterson, G.A. Moses, "MFP - A Calculation of Radiation Mean Free Paths, Ionization, and Internal Energies in Noble Gases," Univ. of Wisconsin Fusion Engineering Program Report UWFDM-307, Sept. 1979.